Evolutionary coexistence in a fluctuating environment by specialization on resource level

Meike T. Wortel[1,*]

[1]Molecular Microbiology and Food Safety, Swammerdam Institute for Life Sciences, University of Amsterdam, Amsterdam, The Netherlands
[*]m.t.wortel@uva.nl

Abstract

Microbial communities in fluctuating environments can contain many species and diversity within species, both in natural environments such as the human gut, and in laboratory settings when communities are propagated for a long time. Whether this diversity is at the species level, within the species level, or a combination of both, the question remains: what processes lead to the origination and maintenance of this diversity?

When nutrient levels fluctuate over time, one possibly relevant process is that different types specialize on low and high nutrient levels. The relevance of this process is supported by observations of types co-existing through this mechanism when put together in the laboratory, and simple models, which show that negative frequency dependence of two types, specialized on low and high resource level, can stabilize coexistence. However, when microbial populations are in an environment for a long time, they will evolve. In this article we determine what happens when species can evolve; whether branching can occur to create diversity and whether evolution will destabilize coexistence.

We find that for the trade-off data between growth at low and high substrate concentrations, available for the bacterium *Escherichia coli* and the yeast *Saccharomyces cerevisiae* on glucose, there is only a small portion of the trait-space that allows for coexistence. Moreover, this coexistence is destabilized by evolution, and the only evolutionary stable outcome is a single strategy. When we combine two species that are well-adapted on their own, we do find that they can form an evolutionary singular coalition. We conclude that although specialization on resource level can support diversity within a species, it is likely not a cause by itself. In contrast, for species consortia this specialization can lead to evolutionary stable coexistence.

1 Introduction

Bacterial species are very abundant on almost all places on earth. Classical theory predicts that only as many species can coexist as there are resources. However, we find many more species. Recently, we observe that there is much more diversity even, as different strains of the same species can exist for long timescales. This happens in complicated environments such as the human gut microbiome [1,2]. More surprisingly, even in laboratory environments, where the environment is simplified as much as possible, we see that long-term coexistence of different clades is very widespread, such as in the Long Term Evolution Experiment [3]. Several explanations have been given for the coexistence in this environment: A type of cross-feeding and enhanced growth in stationary phase and use a of different resource, citrate, that was added as an anti-foaming agent. Since the culture protocol with daily transfers causes fluctuating resource levels, the questions remains if only specialization on the different resource levels can already explain a part of the diversity we observe. This paper therefore investigates the theoretical possibility of evolutionary coexistence of different strains and species on fluctuating resource levels. Although the mathematical framework is adapted to the laboratory experimental evolution protocol of regular transfers to environments with new nutrients, nutrient fluctuations are very abundant in natural systems, and therefore conclusions on coexistence can provide possible explanations for the diversity found in natural systems.

The first observation of coexistence of two strains in an environment with a fluctuating resource level is by Levin [4]. With a mathematical toy model they showed that, when one species takes up nutrients faster at low resource levels and the other at high, coexistence is possible [5]. An extension of the model with fixed cycle lengths and lag phases also shows possibilities of coexistence [6]. In a different experiment, Turner et al. [7] observed coexistence and found evidence of a trade-off on growth at different resource levels, but a mathematical model showed that this was not enough to sustain coexistence. Closer analysis showed that indeed, in addition to the growth trade-off, there was cross-feeding between the strains. These studies are all restricted to analysing strains with fixed properties. To observe coexistence of cohabiting cells, the coexitence should have some evolutionary stability, e.g. adaptation should not lead to the loss of the coexistence.

Fitness in serial transfer cultures consist of many properties, such as lag phase, exponential growth rate, substrate limited growth and death rate. Manhart et al. [8] studies lag phase and exponential growth rate and the evolutionary consequences, such as coexistence and bi-stability and provides a theoretical frame-work for incorporating such measurements. They focus on competitions of sets of strains, and less on evolutionary trajectories.

Coexistence in fluctuating environments by specialization on resource level has been studied and observed, but those papers assume stable properties of the different species, leading to 'ecological coexistence'. This implies that as long as the species do not adapt, they will coexist. However, microorganisms often grow fast and are in large numbers, therefore there is abundant opportunity for adaptation. The assumption that species do not change is not very realistic and it is important to look at the 'evolutionary stable coexistence', where selection on the traits of the different species does not lead to loss of the coexistence. This study addresses the evolutionary trajectories and outcomes in fluctuating environments. To study evolutionary coexistence we need to have knowledge about the possible attainable phenotypes and subsequently use methods that can predict evolutionary trajectories. Here we use adaptive dynamics to investigate the evolutionary coexistence of different strains or species specialized on resource level in a fluctuating environment.

In this paper, we study explicitly evolutionary trajectories, not only fixed strains, using trade-offs supported by experimental data. We focus on growth at different resource levels, which is a nonlinear property (instead of e.g. yield and lag-time), and therefore mathematically more difficult to analyse. First, we show an analytical derivation of the selection pressure. Then, we investigate the evidence and formulas for experimental trade-offs between maximal growth rate an affinity. Next, we study the possible ecological coexistence for such strains and finally evolutionary coexistence, while broadening to multiple species.

2 Model description

The model simulates an environment where the resource is consumed, and at the moment the resource is completely consumed, cells are diluted to a fixed population size and new resource is added. This relates to the conditions that are usually used for experimental evolution, but there are some simplifications. In those conditions cells usually have 4 phases: (1) lag phase, (2) exponential growth, (3) low-nutrient growth and (4) stationary phase[9]. In this paper we only focus on the growth phases (2) and (3).

We assume Monod-growth and calculate the growth over a complete batch cycle. In this way we can calculate the selection gradient and we link this to experiments with a repeated transfer set-up.

2.1 Basic model

First we describe the model for one species (x in concentration) and one substrate (s in concentration). We assume Monod growth with a monod constant k_S (in concentration) and a maximal growth rate μ_{max} (in 1/time). The numerical yield of the species x on the substrate s is $Y_{X/S}$. This leads to the dynamical system:

$$\begin{aligned} \frac{dx(t)}{dt} &= \mu_{max}\frac{s(t)}{k_S + s(t)}x(t) \\ \frac{ds(t)}{dt} &= -\frac{1}{Y_{X/S}}\mu_{max}\frac{s(t)}{k_S + s(t)}x(t) \end{aligned} \tag{1}$$

To enhance readability for the derivations, we will use a notation where we write s and x for $s(t)$ and $x(t)$, μ for μ_{max}, k for k_S and y for $Y_{X/S}$:

$$\begin{aligned} \frac{dx(t)}{dt} &= \mu\frac{s(t)}{k + s(t)}x(t) \\ \frac{ds(t)}{dt} &= -\frac{1}{y}\mu\frac{s(t)}{k + s(t)}x(t) \end{aligned} \tag{2}$$

When we have multiple species or strains (we will call them types), the systems for n types becomes:

$$\begin{aligned} \frac{dx_i}{dt} &= \mu_i\frac{s}{k_i + s}x_i \\ \frac{ds}{dt} &= -\sum_{i=1}^{n}\frac{1}{y_i}\mu_i\frac{s}{k_i + s}x_i \end{aligned} \tag{3}$$

2.2 Growth conditions, fitness and selection gradient

We study the conditions where periodically substrate is added to the system, and cells are diluted to a fixed concentration. To focus solely on the growth phases, we study the system until the substrate runs out, and we stop when $s(t) = 0$. This is equivalent to transferring at long enough timescales such that all substrate is consumed, when there is no death at stationary phase. Death at stationary phase is observed, and trade-offs with for example maximal growth rate are possible, but here we want to isolate the effects of only the growth phases.

Initially, we start every cycle of substrate addition with $s(0) = s_0$ and $\sum_{i=1}^{n} x_i(0) = x_0$. Selection here acts on the increase of growth over a full cycle. We therefore define the final concentration divided by the initial concentration ($x_{i,\infty}/x_{i,0}$) as the growth factor. For one type, at the end of the growth $s(t = end) = 0$ and $x(t = end) = x_0 + ys_0$ and therefore the growth factor is equal to $\frac{x_0+ys_0}{x_0}$.

When we define the fitness, we have to assess the growth factor of a mutant (x^*) with a different monod constant (k^*), maximal growth rate (μ^*) and/or yield (y^*). If the mutant has a higher growth factor than the resident (x), the mutant increases in relative abundance and will be able to invade. More precisely, a mutant can invade when:

$$\frac{x^*(\infty)}{x^*(0)} > \frac{x(\infty)}{x(0)} \tag{4}$$

We define the fitness (W) of the mutant (similar to e.g.[10]) as:

$$W = \frac{\ln(x^*_\infty/x^*_0)}{\ln(x_\infty/x_0)} \tag{5}$$

In evolutionary analysis, the selection coefficient is used. The selection coefficient s is defined as $W - 1$ and therefore a selection coefficient of 0 means that a mutant is not selected for or against (this is equivalent to the definition of $s^* = \ln(x^*_\infty/x_\infty) - \ln(x^*_0/x_0)$[11] also used in[12]). Strains with positive selection coefficients in a resident population will increase in number when rare, and can invade.

By studying the effect of the different phenotypes (in our case μ, k and y) on the fitness, we can calculate the selection gradient. The definition of the selection gradient of a property X is (as in[9]):

$$\frac{x}{W}\frac{\partial W}{\partial X} \tag{6}$$

2.3 Evolutionary optimum, evolutionary stable strategies (ESS) and evolutionary singular coalitions (ESC)

Since the properties of a type define the ecological properties, in this case the substrate level over time, we cannot directly define the evolutionary optimum. According to evolutionary game theory, we define the optimum here as the evolutionary stable strategy (ESS). Therefore we look at a strategy (μ, k, y) that cannot be invaded by any other strategy (there is no strategy with a positive selection coefficient: $\nexists(\mu^*, k^*, y^*) : s > 0$). When the properties are unbounded, there is no answer to this question, but in practice the properties are bounded and correlated. Trade-offs between these properties can lead to an evolutionary stable strategy or evolutionary singular coalitions. Although in theory evolutionary singular coalitions of more than two types are possible, the scenarios discussed in this paper will never lead to such coalitions, and therefore we further restrain to coalitions of two types.

Stable coexistence requires for both types have to invade a monoculture of the other type (frequency dependent selection). In this system that would happen when one type specialises on high resource (high growth rate on high resource) and therefore reduces the high resource phase when abundant, while the other type specialises on low resource and reduces that phase when abundant. This leads to stable coexistence of the two types as long as there are no evolutionary changes, which I will further refer to as ecological coexistence.

When we do allow for evolutionary changes, ecological coexistence could become destabilized. When the coexistence is stable even under evolutionary changes, I will refer to it as evolutionary coexistence, which leads to evolutionary singular coalition (ESC) defined in adaptive dynamics[13]. We will use adaptive dynamics techniques to find conditions where we have ECSs. Traditionally, adaptive dynamics assumes an ecological timescale and an evolutionary timescale, and assumes the ecological timescale to be in steady state when assessing the evolutionary dynamics. In this system, the ecological timescale coincides with the dynamics over the coarse of many transfers, and the evolutionary timescale where we assess property changes, assumes that the ecological timescale is in steady state, therefore the profile within a transfer is the same from transfer to transfer. Our system includes a third timescale, the rapid timescale, which encompasses the changes within a transfer.

3 Results

3.1 Fitness function

The invasion fitness of the mutant is (see section A.2 for the derivation):

$$W^* = \frac{\ln(x^*_\infty/x^*_0)}{\ln(x_\infty/x_0)} = \frac{\ln\left[\left(\frac{k^*+s_0}{k^*}\right)^{\frac{\mu^*}{\mu}\frac{k-k^*}{k^*+\frac{x_0}{y}+s_0}}\left(\frac{x_0+ys_0}{x_0}\right)^{\frac{\mu^*}{\mu}\frac{k+\frac{x_0}{y}+s_0}{k^*+\frac{x_0}{y}+s_0}}\right]}{\ln\left[\frac{x_0+ys_0}{x_0}\right]} \tag{7}$$

We see that if $\mu^* = \mu$ and $k^* = k$, the growth factor of the mutant ($\frac{x^*(\infty)}{x^*(0)}$) is exactly that of the resident ($\frac{x_0+ys_0}{x_0}$) and $W^* = 1$. If $k^* = k$ and $\mu^* \neq \mu$, the growth factor of the mutant is the growth factor of the resident to the power $\frac{\mu^*}{\mu}$ and the invasion fitness is $\frac{\mu^*}{\mu}$. The effect of $k^* \neq k$ is more difficult to see in the equation, as well as the effect of a trade-off between μ and k. It can be seen that a mutant with a higher μ^* and a higher k^* benefits from long periods of high nutrients, that is a high s_0 and a low x_0. Indeed, it follows from the above equation that a high s_0 leads to a relatively stronger effect of μ^* on the growth factor (and therefore a higher invasion fitness) while a high x_0 leads to a relatively larger effect of k^*.

The numerical yield is not relevant for the fitness of an invading strain, as we can scale x_0 with the yield and make it 1. The growth rate might be affected by the yield, but that effect could be added as a tradeoff between the parameters μ, k and y. There is no selection on y but any result that is affected by x_0 is inversely affected by y. However, the yield of the resident strain does affect the fitness of other invading mutants. For the evolutionary analysis we will use the selection coefficient (s) instead of the invasion fitness:

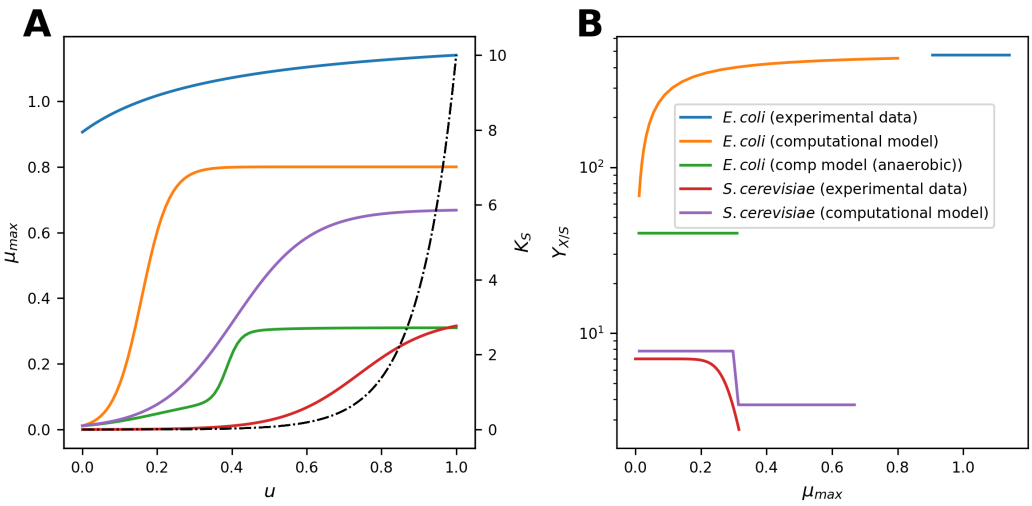

Figure 1: Trade-offs between growth parameters. **A** Trade-offs between μ_{max} and k_S given as function of the introduced specialization parameter u, which scales logarithmically with k_S (dashed line). **B** Trade-offs between $Y_{X/S}$ and μ_{max} that are related to the data used for the trade-offs in part **A**.

$$s = W^* - 1 = \frac{\ln\left[\left(\frac{k^*+s_0}{k^*}\right)^{\frac{\mu^*}{\mu}\frac{k-k^*}{k^*+\frac{x_0}{y}+s_0}}\left(\frac{x_0+ys_0}{x_0}\right)^{\frac{\mu^*}{\mu}\frac{k+\frac{x_0}{y}+s_0}{k^*+\frac{x_0}{y}+s_0}}\right]}{\ln\left[\frac{x_0+ys_0}{x_0}\right]} - 1 \tag{8}$$

3.2 Trade-off in growth parameters for *Escherichia Coli* and *Saccharomyces Cerevisiae*

Evolutionary dynamics can be interesting when the growth properties are bounded, or there is a trade-off between the properties. Since there is no selection on the numerical yield, we first investigate a trade-off between the μ_{max} and k_S. A possible mechanism behind this trade-off could be a protein investment trade-off, e.g. the cell can invest in transporters to improve growth on low resource levels or the cell can invest in ribosomes to improve growth at high substrate levels. To model this trade-off, information about the evolutionary potential of cells with regard to μ_{max} and k_S are required, which are difficult to come by. We have collected some data for *E. coli*[14] and *S. cerevisiae*[15]. A different approach is to use a mechanistic computational model, optimize it under different external substrate concentrations, and then derive the μ_{max} and k_S. We included this method for these same species, and for *E. coli* we included anaerobic conditions[16,17]. Note that in some cases the trade-off is related to transport kinetics[15], but mostly it is a property of the whole cell and surfaces even with a single transporter. The resulting trade-offs are shown in figure 1A (see Appendix A.3 for details on the fitting of the curves).

There is no direct selection on the yield, but the yield affects the dynamics of substrate depletion, and therefore the environment for other species. There is quite some literature on trade-offs between μ_{max} and $Y_{X/S}$ (see Beardmore et al.[18] for a summary), but here we used yields from the same sources as the other growth parameters as much as possible. See Figure 1B for the implemented yields.

3.3 Ecological coexistence and evolutionary stable strategies

We next wonder whether we could expect coexistence of well-adapted strains, where one strain is more adapted to low nutrients, while the other is more adapted to high nutrients. For this coexistence to be stable, the strains need to have a negative frequency dependent fitness (i.e. their fitness is lower the more abundant they are). There is indeed a negative frequency dependent effect, because the more abundant a high-substrate specialist is, the faster the substrate is depleted when it is high, and therefore the shorter the period of high substrate (and similarly for the low-substrate specialist). Since the highest fitness is when a type is rare, we can find coexistence by studying mutual invasability.

To study this behaviour of invasion of new types, and to find types that cannot be invaded, we use pairwise invasibility plots (PIPs) of adaptive dynamics. To construct these, we have to define the types by a one-dimensional parameter. Since types that are not on the trade-off line of μ_{max} and k_S can always be invaded by a type with the same μ_{max} and a lower k_S, or the same k_S and a higher μ_{max}, we can assume all types are on the trade-off line. We defined a new property, u, which specifies specialization on low to high resource levels on a scale of 0 to 1, and assigns a μ_{max} and k_S to every value of u. The yields are not explicitly mentioned, but they change with u (see Figure 1B and Appendix Section A.3).

When we construct this PIP for *E. coli* under conditions commonly used for repeated transfer experiment, we observe that there is a single evolutionary stable strategy (see Figure 2A). If the resident would be very

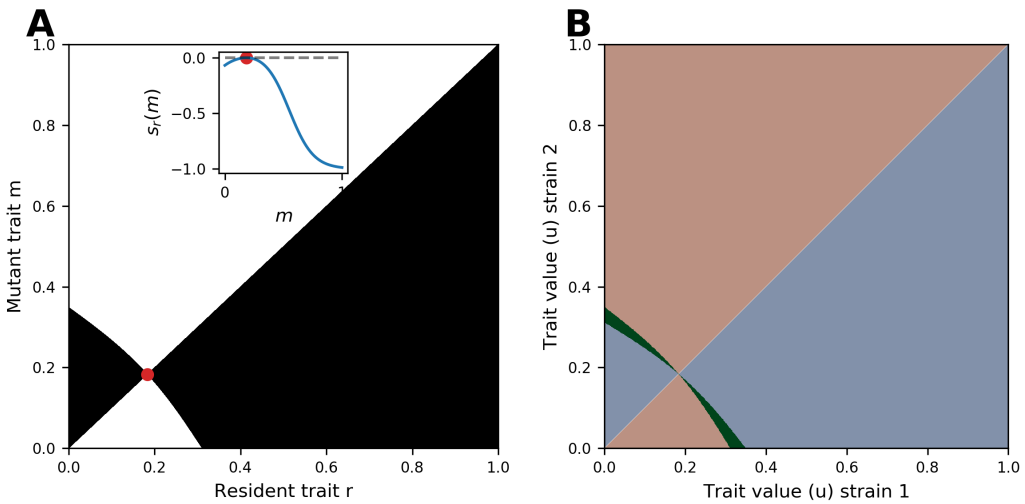

Figure 2: **Invasion potential of different strategies. A** Pairwise invasibility plot for the experimentally derived trade-off for *E. coli* at the conditions of the LTEE (initial glucose = 0.1375 mM, initial cells are $0.5{\cdot}10^6$ cells/ml)[9]. The inset shows that the equilibrium is invasion stable. It is also attracting and therefore an ESS. **B** Mutual invasibility plot. By flipping the PIP of **A** and overlaying it with the PIP, we can determine the area of mutual invasibility and therefore ecological coexistence.[13]

adapted to low substrate (low u), higher substrate specialists can invade, and if the resident is adapted to higher substrate (high u), lower substrate specialists can invade. In the ESS, no other type can invade (see inset in 2A). We can overlay this PIP with it's mirror, to see when two types can mutually invade (green area in 2B).

This is for one species, with one approximated trade-off and under one condition. Since we have an analytical expression for the selection coefficient, we can investigate many scenarios. However, for all trade-offs, from experimental and computational data, the general picture looks the same (see Appendix Section A.5): There is a small area of ecological co-existence, but this coexistence is not evolutionary stable and the only attracting point is a single-type ESS. This means that two strains adapted to different conditions, such as a high-nutrient and low-nutrient condition, could coexist when placed together in a serial transfer culture. However, if we let them then adapt in the same regime, they will evolve in such a way, that one of the strains will be lost, and we will end up with a single strain.

3.4 Evolutionary coexistence in multiple species consortia

In the previous section we showed that there are cases in which there are two types that will coexist in the coarse of continued transfers. However, we mostly expect to observe coexisting types if the coexistence is not destabilized by evolution. We have not found this for a single species, but were we limited to only two well-studied species, a single substrate and few approximations of the trade-offs. It is possible that evolutionary coexistence could be found for different species, although the observed trend does not make this very likely. Now we investigate whether we can use a similar approach to investigate if evolutionary stable coexistence is possible in species consortia.

We first combine two trade-offs in a single one, which is only possible when the trade-off curves intersect (see Figure 1). We will therefore model a co-culture of *E. coli* and *S. cerevisiae* under anaerobic conditions, and will use the computational trade-off for *E. coli* and the experimental trade-off for *S. cerevisiae* to illustrate this method. First we have to construct a new trade-off that combines the two (see Figure 3A and B and Appendix Section A.3.5). Of course one species cannot convert into another one by evolutionary change at the studied timescale, therefore we should discard mutations that cross the intersection of the trade-off curves. However, since this intersection is in a fitness minimum, this is almost guaranteed to not happen.

When we construct the pairwise invasibility plot for the two-species trade-off, there are three equilibria, one local minimum at the species intersection and two local maxima, one for each species (Figure 3C). The single species maxima are both ESSes and will be reached when we start with a single species (Figure 4 and Appendix Figure A.6). With the same methods as before we can show there is an area of mutual invasibility between the species, shown as the green area in Figure 4. As can be seen, if both species would be adapted alone under these conditions, the would coexist when placed together. Moreover, using the analysis of trait evolution plots, we can show that there is an evolutionary attracting point in the species coexistence area[13]. With simulations (Appendix Figure A.6) we can find this point and we show numerically that in this point, the selection coefficient for all other types is negative (inset in Figure 4). This means that after the species coexist together, they will continue to evolve, but reach an evolutionary stable coexistence or evolutionary singular coalition (ESC).

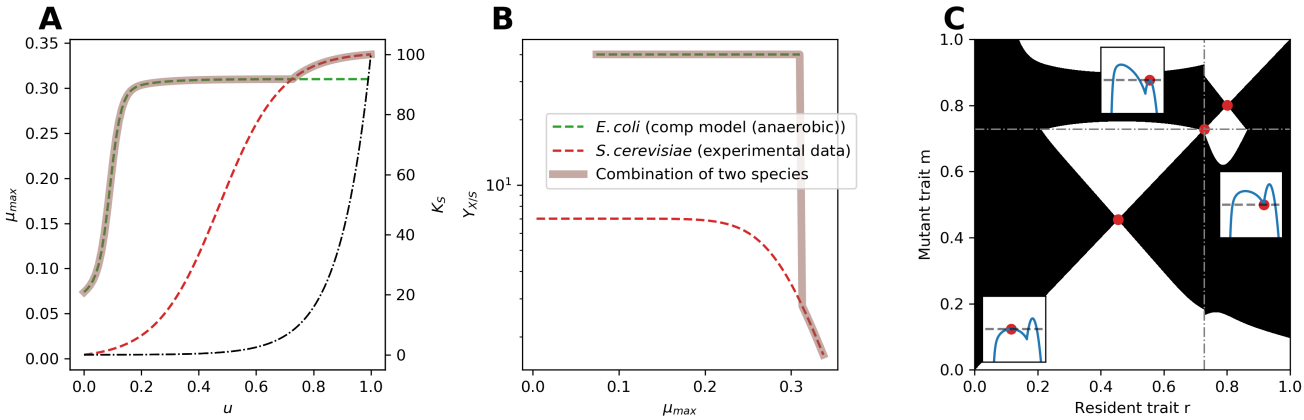

Figure 3: **Combined trade-off of two species. A** Again transformation to the specialization parameter u is used, which now signifies k_S from 0.01 to 100. The maximum of the μ_{max} of the two species is used for this combined trade-off. **B** The yield corresponding to the species from which the trade-off is takes is used for the yield of the combined trade-off. **C** In the PIP we can see there are three equilibria, of which the middle one is a local minimum corresponding to the switching point of one species to the other (gray dashes lines; those cannot be crossed by mutations). There are two equilibria that are attracting and locally invasion stable, which correspond to the ESS for each species.

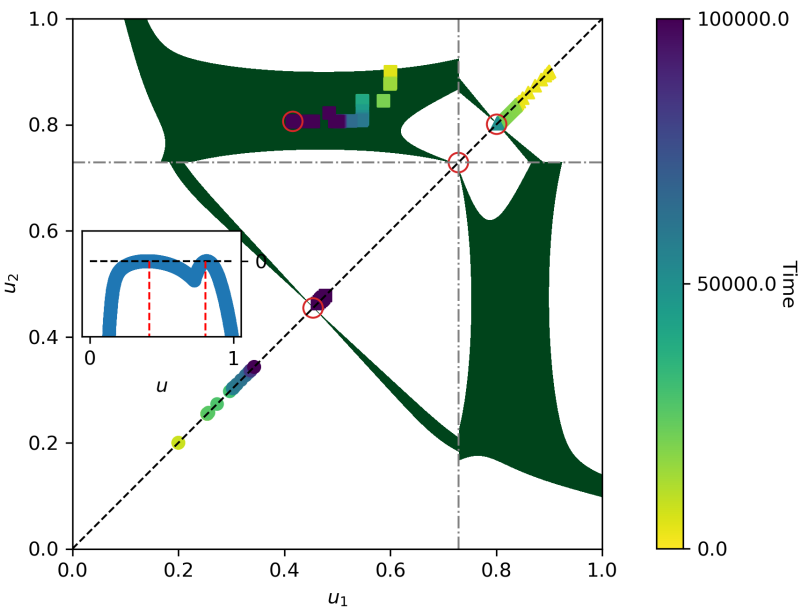

Figure 4: **An evolutionary singular coalition of two species.** Three different simulations are plotted onto the area of coexistence, created with the mutual invasibility plot (see Appendix Figure A.6 for the simulations). When initially one species is present, a single species ESS is reached. However, when we start with two species within the area of coexistence, an evolutionary singular coalition (ESC) is reached. As shown in the inset, when in this ESC all other types have a negative selection coefficient, and therefore this ESC is evolutionary stable.

4 Discussion

Nutrient fluctuations can be imposed in the laboratory, or arise from environmental processes. In this paper we show that specialization on resource level in such fluctuating environments is not likely to lead to diversity within a species as a single or major cause, because while coexistence is possible, it will be destabilized by evolution. However, the same process can achieve evolutionary stable coexistence between multiple species in a community.

Experimental observation do suggest that strains can coexist by specializing on nutrient level[4,7]. It is likely only part of one of more factors causing co-existence, such as in Turner et al.[7], where this specialization is combined with cross-feeding.

We have used a trade-off between maximal growth rate and substrate affinity to determine the possible trait space of the organisms. We have shown some support for this trade-off, however Velicer and Lenski[19] set out to measure this trade-off experimentally and found more contra- than supporting evidence. However, as they also note, perhaps their experiment was not long enough to actually reach the trade-off, and general growth performance mutations on the supplied substrate were selected for.

We have only discussed the co-existence of two strains or species. Previous studies have shown theoretically more than two species could coexist, albeit mostly though numerical simulations or only showing neutral co-existence[5,6,12]. However, because of the way species are designed and the experimental data on trade-offs we present here, more than two strains stable coexisting is in reality likely not feasible. Still, if specialization on an intermediate level of resource is a side-effect, it can still help a new variant (temporally) gain some benefit.

In conclusion, we have shown that we can use adaptive dynamics and trade-offs based on experimental data to show the biologically relevance of an observed and suggested mechanism behind diversity of microbial communities in fluctuating environments. As more quantitative data becomes available and more mechanistic models can be parameterized, we can investigate how common it is that species could coexist by specialization on resource level. Moreover, some conditions and species could lead to trade-offs that do allow for evolutionary stable diversity within a species, and here we supply the techniques to investigate that.

5 Acknowledgements

I would like to thank Han Peters for help with the mathematical derivations, Hans Metz for help with applying adaptive dynamics techniques, Guilhem Doulcier for the online availability of his lecture notes and code on adaptive dynamics and Juan Bonachela, Bob Planqué, Martijn Egas and Huub Hoefsloot for helpful discussions.

References

[1] Nandita R. Garud, Benjamin H. Good, Oskar Hallatschek, and Katherine S. Pollard. Evolutionary dynamics of bacteria in the gut microbiome within and across hosts. *PLOS Biology*, 17(1):e3000102, January 2019. ISSN 1545-7885. doi: 10.1371/journal.pbio.3000102. URL `https://dx.plos.org/10.1371/journal.pbio.3000102`.

[2] Shijie Zhao, Tami D. Lieberman, Mathilde Poyet, Kathryn M. Kauffman, Sean M. Gibbons, Mathieu Groussin, Ramnik J. Xavier, and Eric J. Alm. Adaptive Evolution within Gut Microbiomes of Healthy People. *Cell Host & Microbe*, 25(5):656–667.e8, May 2019. ISSN 19313128. doi: 10.1016/j.chom.2019.03.007. URL `https://linkinghub.elsevier.com/retrieve/pii/S1931312819301593`.

[3] Benjamin H. Good, Michael J. McDonald, Jeffrey E. Barrick, Richard E. Lenski, and Michael M. Desai. The dynamics of molecular evolution over 60,000 generations. *Nature*, 551(7678):45–50, November 2017. ISSN 1476-4687. doi: 10.1038/nature24287. Number: 7678 Publisher: Nature Publishing Group.

[4] Bruce R. Levin. Coexistence of Two Asexual Strains on a Single Resource. *Science*, 175(4027): 1272–1274, March 1972. ISSN 0036-8075, 1095-9203. doi: 10.1126/science.175.4027.1272. URL `https://science.sciencemag.org/content/175/4027/1272`. Publisher: American Association for the Advancement of Science Section: Reports.

[5] Frank M. Stewart and Bruce R. Levin. Partitioning of Resources and the Outcome of Interspecific Competition: A Model and Some General Considerations. *The American Naturalist*, 1973. ISSN 0003-0147. doi: 10.1086/282825. URL `https://www.journals.uchicago.edu/doi/abs/10.1086/282825`. Publisher: University of Chicago Press.

[6] Hal L. Smith. Bacterial competition in serial transfer culture. *Mathematical Biosciences*, 229(2):149–159, February 2011. ISSN 0025-5564. doi: 10.1016/j.mbs.2010.12.001. URL `https://www.sciencedirect.com/science/article/pii/S0025556410001811`.

[7] Paul E. Turner, Valeria Souza, and Richard E. Lenski. Tests of Ecological Mechanisms Promoting the Stable Coexistence of Two Bacterial Genotypes. *Ecology*, 77 (7):2119–2129, 1996. ISSN 1939-9170. doi: https://doi.org/10.2307/2265706. URL `https://esajournals.onlinelibrary.wiley.com/doi/abs/10.2307/2265706`. _eprint: https://esajournals.onlinelibrary.wiley.com/doi/pdf/10.2307/2265706.

[8] Michael Manhart, Bharat V. Adkar, and Eugene I. Shakhnovich. Trade-offs between microbial growth phases lead to frequency-dependent and non-transitive selection. *Proceedings of the Royal Society B: Biological Sciences*, 285(1872):20172459, February 2018. doi: 10.1098/rspb.2017.2459. URL `https://royalsocietypublishing.org/doi/10.1098/rspb.2017.2459`. Publisher: Royal Society.

[9] Farida Vasi, Michael Travisano, and Richard E Lenski. Long-term experimental evolution in Escherichia coli. II. Changes in life-history traits during adaptation to a seasonal environment. *The american naturalist*, 144(3):432–456, 1994. Publisher: University of Chicago Press.

[10] Michael J Wiser, Noah Ribeck, and Richard E Lenski. Long-term dynamics of adaptation in asexual populations. *Science*, 342(6164):1364–1367, 2013. Publisher: American Association for the Advancement of Science.

[11] Luis-Miguel Chevin. On measuring selection in experimental evolution. *Biology Letters*, 7(2):210–213, April 2011. doi: 10.1098/rsbl.2010.0580. URL `https://royalsocietypublishing.org/doi/10.1098/rsbl.2010.0580`. Publisher: Royal Society.

[12] Michael Manhart and Eugene I. Shakhnovich. Growth tradeoffs produce complex microbial communities on a single limiting resource. *Nature Communications*, 9(1):3214, August 2018. ISSN 2041-1723. doi: 10.1038/s41467-018-05703-6. URL `https://www.nature.com/articles/s41467-018-05703-6`. Number: 1 Publisher: Nature Publishing Group.

[13] S.A.H. Geritz, E. Kisdi, G. MeszeNA, and J.A.J. Metz. Evolutionarily singular strategies and the adaptive growth and branching of the evolutionary tree. *Evolutionary Ecology*, 12(1):35–57, January 1998. ISSN 1573-8477. doi: 10.1023/A:1006554906681. URL `https://doi.org/10.1023/A:1006554906681`.

[14] Kai W Wirtz. A generic model for changes in microbial kinetic coefficients. *Journal of Biotechnology*, 97 (2):147–162, 2002. Publisher: Elsevier.

[15] Karin Elbing, Christer Larsson, Roslyn M. Bill, Eva Albers, Jacky L. Snoep, Eckhard Boles, Stefan Hohmann, and Lena Gustafsson. Role of Hexose Transport in Control of Glycolytic Flux in Saccharomyces cerevisiae. *Applied and Environmental Microbiology*, 70(9):5323–5330, September 2004. ISSN 0099-2240, 1098-5336. doi: 10.1128/AEM.70.9.5323-5330.2004. Publisher: American Society for Microbiology Section: PHYSIOLOGY AND BIOTECHNOLOGY.

[16] Meike T. Wortel, Elad Noor, Michael Ferris, Frank J. Bruggeman, and Wolfram Liebermeister. Metabolic enzyme cost explains variable trade-offs between microbial growth rate and yield. *PLOS Computational Biology*, 14(2):e1006010, February 2018. ISSN 1553-7358. doi: 10.1371/journal.pcbi.1006010. Publisher: Public Library of Science.

[17] Meike T. Wortel, Evert Bosdriesz, Bas Teusink, and Frank J. Bruggeman. Evolutionary pressures on microbial metabolic strategies in the chemostat. *Scientific Reports*, 6(1):29503, July 2016. ISSN 2045-2322. doi: 10.1038/srep29503. Number: 1 Publisher: Nature Publishing Group.

[18] Robert E. Beardmore, Ivana Gudelj, David A. Lipson, and Laurence D. Hurst. Metabolic trade-offs and the maintenance of the fittest and the flattest. *Nature*, 472(7343):342–346, April 2011. ISSN 0028-0836, 1476-4687. doi: 10.1038/nature09905.

[19] Gregory J. Velicer and Richard E. Lenski. Evolutionary Trade-Offs Under Conditions of Resource Abundance and Scarcity: Experiments with Bacteria. *Ecology*, 80(4):1168–1179, 1999. ISSN 1939-9170. doi: https://doi.org/10.1890/0012-9658(1999)080[1168:ETOUCO]2.0.CO;2.

[20] Meike T. Wortel, Han Peters, Josephus Hulshof, Bas Teusink, and Frank J. Bruggeman. Metabolic states with maximal specific rate carry flux through an elementary flux mode. *The FEBS Journal*, 281(6):1547–1555, 2014. ISSN 1742-4658. doi: https://doi.org/10.1111/febs.12722. URL `https://febs.onlinelibrary.wiley.com/doi/abs/10.1111/febs.12722`. _eprint: https://febs.onlinelibrary.wiley.com/doi/pdf/10.1111/febs.12722.

[21] Johan H. van Heerden, Meike T. Wortel, Frank J. Bruggeman, Joseph J. Heijnen, Yves J. M. Bollen, Robert Planqu, Josephus Hulshof, Tom G. O'Toole, S. Aljoscha Wahl, and Bas Teusink. Lost in transition: start-up of glycolysis yields subpopulations of nongrowing cells. *Science (New York, N.Y.)*, 343(6174):1245114, February 2014. ISSN 1095-9203. doi: 10.1126/science.1245114.

[22] Heinrich Senn, Urs Lendenmann, Mario Snozzi, Geoffrey Hamer, and Thomas Egli. The growth of Escherichia coli in glucose-limited chemostat cultures: a re-examination of the kinetics. *Biochimica et Biophysica Acta (BBA)-General Subjects*, 1201(3):424–436, 1994. Publisher: Elsevier.

A Appendix

A.1 Parameters and variables

Symbol	Name	Units
x	Biomass	10^6 cells ml^{-1}
s	Substrate	mM
μ or μ_{max}	Maximal growth rate	h^{-1}
k or k_S	Monod constant (substrate at half maximal growth)	mM
y or $Y_{X/S}$	Yield of biomass on substrate	10^9 cells mmol^{-1}

A.2 Derivation of the mutant fitness and the selection gradients

To find a fitness of a mutant (x^*), we need to calculate how it increases in frequency when it invades in the population of a resident (x). We will assume that this mutant is in such a small amount that the mutant does not affect the metabolite profile $s(t)$. Then, we will deduce the growth factor ($\frac{x^*(\infty)}{x^*(0)}$) for the mutant. For the derivations we will use the notation of (2).

$$\begin{aligned} \frac{dx^*}{dt} &= \mu^* \frac{s}{k^*+s} x^* \\ \frac{1}{x^*}\frac{dx^*}{dt} &= \mu^* \frac{s}{k^*+s} \\ \frac{d}{dt}(\ln x^*) &= \mu^* \frac{s}{k^*+s} \end{aligned} \tag{9}$$

Note that the right hand side depends on t but not on x^*, because we assumed that the metabolite profile is determined by the resident. Thus:

$$\begin{aligned} \ln(x^*(\infty)) - \ln(x^*(0)) &= \int_0^\infty \mu^* \frac{s}{k^*+s} dt \\ \frac{x^*(\infty)}{x_0^*} &= e^{\int_0^\infty \mu^* \frac{s}{k^*+s} dt} \end{aligned} \tag{10}$$

To calculate the above integral we change variables from $s(t)$ to s. Because we know that s runs from s_0 to 0, we integrate from s from s_0 to 0 in stead of t from 0 to ∞. We do have to multiply with the derivative $\frac{dt}{ds}$:

$$\int_0^\infty \mu^* \frac{s(t)}{k^*+s(t)} dt = \int_{s_0}^0 \mu^* \frac{s}{k^*+s} \frac{dt}{ds} ds \tag{11}$$

We can calculate $\frac{dt}{ds}$ from equations (2). First we express x in s and constants:

$$\begin{aligned} x(t) - x(0) &= y(s(0) - s(t)) \\ x(t) &= y(s_0 - s(t)) + x_0 \end{aligned} \tag{12}$$

Then we can work out $\frac{ds}{dt}$:

$$\begin{aligned} \frac{ds}{dt} &= -\frac{1}{y}\mu \frac{s}{k+s} x \\ &= -\frac{1}{y}\mu \frac{s}{k+s}(y(s_0 - s) + x_0) \\ &= -\mu \frac{s(\frac{x_0}{y} + s_0 - s)}{k+s} \end{aligned} \tag{13}$$

Then we get:

$$\frac{dt}{ds} = -\frac{1}{\mu} \frac{k+s}{s(\frac{x_0}{y} + s_0 - s)} \tag{14}$$

Now we can use equation (14) to calculate the integral (11):

$$\begin{aligned} \int_{s_0}^0 \mu^* \frac{s}{k^*+s} \frac{dt}{ds} ds &= \frac{\mu^*}{\mu} \int_0^{s_0} \frac{k+s}{k^*+s} \frac{1}{\frac{x_0}{y} + s_0 - s} ds \\ &= \frac{\mu^*}{\mu} \left[\frac{k-k^*}{k^* + \frac{x_0}{y} + s_0} \ln(k^*+s) - \frac{k + \frac{s_0}{y} + s_0}{k^* + \frac{s_0}{y} + s_0} \ln(\frac{x_0}{y} + s_0 - s) \right]_{s=0}^{s=s_0} \\ &= \frac{\mu^*}{\mu} \left(\frac{k-k^*}{k^* + \frac{x_0}{y} + s_0} \ln\left(\frac{k^*+s_0}{k^*}\right) + \frac{k + \frac{x_0}{y} + s_0}{k^* + \frac{x_0}{y} + s_0} \ln\left(\frac{x_0 + ys_0}{x_0}\right) \right) \end{aligned} \tag{15}$$

To calculate the growth factor of the mutant ($\frac{x^*(\infty)}{x^*(0)}$), we have to take e to the power the above integral (see equation (10)):

$$\frac{x^*(\infty)}{x_0^*} = \left(\frac{k^*+s_0}{k^*}\right)^{\frac{\mu^*}{\mu} \frac{k-k^*}{k^* + \frac{x_0}{y} + s_0}} \left(\frac{x_0 + ys_0}{x_0}\right)^{\frac{\mu^*}{\mu} \frac{k + \frac{x_0}{y} + s_0}{k^* + \frac{x_0}{y} + s_0}} \tag{16}$$

Using the definition (5), we can describe the fitness as:

$$\frac{\ln(x^*_\infty/x^*_0)}{\ln(x_\infty/x_0)} = \frac{\ln\left[\left(\frac{k^*+s_0}{k^*}\right)^{\frac{\mu^*}{\mu}\frac{k-k^*}{k^*+\frac{x_0}{y}+s_0}}\left(\frac{x_0+ys_0}{x_0}\right)^{\frac{\mu^*}{\mu}\frac{k+\frac{x_0}{y}+s_0}{k^*+\frac{x_0}{y}+s_0}}\right]}{\ln\left[\frac{x_0+ys_0}{x_0}\right]} \tag{17}$$

A.2.1 Constant dilution (d) instead of constant initial biomass (x_0

In the case that we do not start every transfer with a fixed biomass concentration, but instead fix the dilution from one transfer to the next. This means that the biomass at the beginning is equal to the final biomass divided by the dilution factor d:

$$x_0 = \frac{x_{\inf}}{d} \quad = \frac{x_0 + ys_0}{x \quad {}_0} = \frac{ys_0}{d-1} \tag{18}$$

The fitness then becomes:

$$\frac{\ln(x^*_\infty/x^*_0)}{\ln(x_\infty/x_0)} = \frac{\ln\left[\left(\frac{k^*+s_0}{k^*}\right)^{\frac{\mu^*}{\mu}\frac{k-k^*}{k^*+\frac{d}{d-1}s_0}} d^{\frac{\mu^*}{\mu}\frac{k+\frac{d}{d-1}s_0}{k^*+\frac{d}{d-1}s_0}}\right]}{\ln d} \tag{19}$$

A.3 Trade-offs between μ_{max}, k_S and y

A.3.1 *E. coli* from experimental data

A trade-off between maximal growth rate and affinity has been fitted to experimental data[14]:

$$\mu_{max} = \mu^{ref}\frac{log(\frac{k}{k^{ref}})}{log(\frac{k}{k^{ref}})+1} \tag{20}$$

There was a small mistake with the parameters reported in the paper (personal communication) and we have converted the parameter k^{ref} from $\mu g\, L^{-1}$ to mM. This results in the parameters $\mu^{ref} = 1.23\, h^{-1}$ and $k^{ref} = 3.056 \cdot 10^{-5}\, mM$. Since we have no information on the yield for this data, we used a constant yield derived from the Long Term Evolution Experiment of $474 \cdot 10^9$ cells mmol^{-1}[9].

A.3.2 *E. coli* from kinetic model of central metabolism

For an actual evolutionary trade-off, we need to find the pareto optimum between different properties. Maximal growth rates and affinities in experimental conditions are usually for cells that are optimized for one of these properties. Another way to approach optimal conditions is by making a computational model of a species and then optimizing the model for different growth properties. We used a model of the central carbon metabolism of *E. coli*[16] for this purpose. Optimal yield and growth under defined external conditions are achieved by elementary flux modes[20], allowing us to find the pareto front by selecting the pareto optimal EFMs. Fitting a function through these pareto optimal EFMs for μ_{max} and k_S, and another function for $Y_{X/S}$ and μ_{max} leads to:

$$\begin{aligned}\mu_{max} &= \mu^{ref}\frac{(k^{ref})^n}{\frac{1}{k}^n + (k^{ref})^n}\\ Y_{X/S} &= y_{max}\frac{\mu_{max}}{\mu_{max}+y_{ref}}\end{aligned} \tag{21}$$

With $\mu^{ref} = 0.8$, $k^{ref} = 417$ and $n = 2.7$ for the first equation and $y_{max} = 495$ and $y_{ref} = 0.0726$ for the second equation. For anaerobic growth we observe a different shape trade-off:

$$\mu_{max} = \mu_1^{ref}\frac{k}{k+k_1^{ref}} + \mu_2^{ref}\frac{k^n}{k^n+(k_2^{ref})^n} \tag{22}$$

With $\mu_1^{ref} = 0.1$, $k_1^{ref} = 3.9 \cdot 10^{-3}$, $\mu_2^{ref} = 0.21$, $k_2^{ref} = 2.3 \cdot 10^{-2}$ and $n = 5.6$. Under anaerobic conditions we observed a relatively constant yield of $40 \cdot 10^9$ cells mmol^{-1}. See Fig. A.1 for the fits.

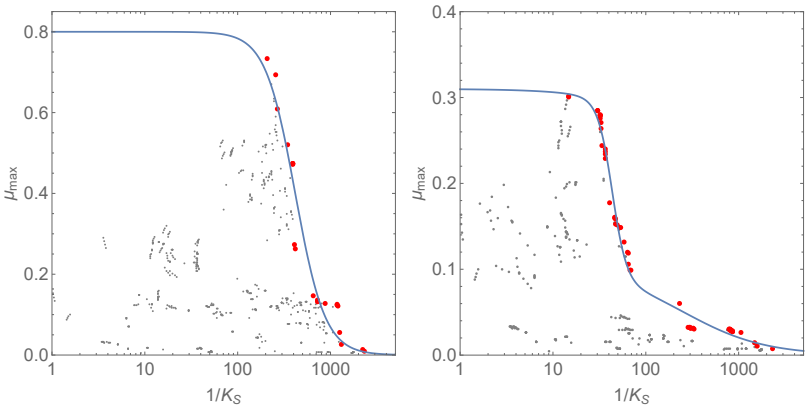

Figure A.1: **Trade-off curves fitted to the pareto front** Left: Aerobic conditions. Right: Anaerobic conditions.

A.3.3 *S. cerevisiae* from experimental data

We used data from *S. cerevisiae* with all glucose transporters knocked out and single transporters or chimeras of two different transporters placed back[15]. The K_M's of the transporters as well as the growth rates are reported for these strains. We checked with a model of *S. cerevisiae* glycolysis[21] and when the transporter K_M is the only difference, this also reflects the substrate concentration of half maximal glycolysis rate. Assuming glycolysis rate is related to growth rate, in this case the K_M of the transporter will be a good proxy for the K_S of the cell. The function for these data is:

$$\begin{aligned} \mu_{max} &= \mu^{ref} \frac{k_S}{k_S + k^{ref}} \\ Y_{X/S} &= y_{max} \frac{y_{ref}^m}{\mu_{max}^m + y_{ref}^m} \end{aligned} \tag{23}$$

With $\mu^{ref} = 0.34$, $k_S = 0.77$, $y_{max} = 7$, $y_{ref} = 0.3$ and $m = 10$.

A.3.4 *S. cerevisiae* from self-replicator model

To overcome the issue that the experimental is on cells that have not be optimized for either μ_{max} or k_S, we also investigated a computational approach to get a trade-off curve for *S. cerevisiae*. We used a self-replicator model that includes all reactions to replicate itself, although in a very simplified form, and is parameterized on experimental data[17]. When we optimize this self-replicator model on different levels of the resource (glucose), and then fit Monod curves through each of the optimized parameters, we obtain different values for μ_{max} and k_S. We fitted a trade-off curve through the corresponding μ_{max} and k_S values and reported the yield:

$$\begin{aligned} \mu_{max} &= \mu^{ref} \frac{k_S}{k_S + k^{ref}} \\ Y_{X/S} &= 7.8 \ \text{ when } \mu_{max} < 0.3 \\ Y_{X/S} &= 3.7 \ \text{ when } \mu_{max} \geq 0.3 \end{aligned} \tag{24}$$

with $\mu^{ref} = 0.67$ and $k^{ref} = 0.028$ (See Figure 1).

A.3.5 Combined trade-off of two species

To investigate evolutionary coexistence of two species while still applying the same analytical and graphical analyses as for the single species case, we can make a single trade-off curve that encompasses the two separate trade-off curves. Because mutations cannot change one species in another, we have to make sure there are no mutations across the species boundary, which is likely if we have the species boundary in a fitness minimum.

To apply this we have combined the experimentally derived trade-off for *S. cerevisiae* (section A.3.3) and the computationally derived trade-off for *E. coli* for anaerobic conditions (section A.3.2). See Figure 3.

A.4 Selection gradient

For μ the selection coefficient (6) is always equal to 1, because eq (7) is proportional to μ^*, the derivative $\partial W/\partial \mu^*$ is exactly W/μ^*. Since we assume the mutant has not influence on the nutrient profile, the selection gradient for y^* is 0. For k^* this selection gradient in the point $k = k^*$ is equal to (we are keeping everything but the k constant, so $\mu^*/\mu = 1$):

$$\frac{k^*}{w}\frac{\partial w}{\partial k^*}(k^* = k) = \frac{-k\left(1 + \frac{\ln\left(\frac{k+s_0}{k}\right)}{\ln\left(\frac{x_0+ys_0}{x_0}\right)}\right)}{k + \frac{x_0}{y} + s_0} \tag{25}$$

The selection gradient S_X for a property X is the proportional partial derivative of the invasion fitness to the property. This leads to the following selection gradients:

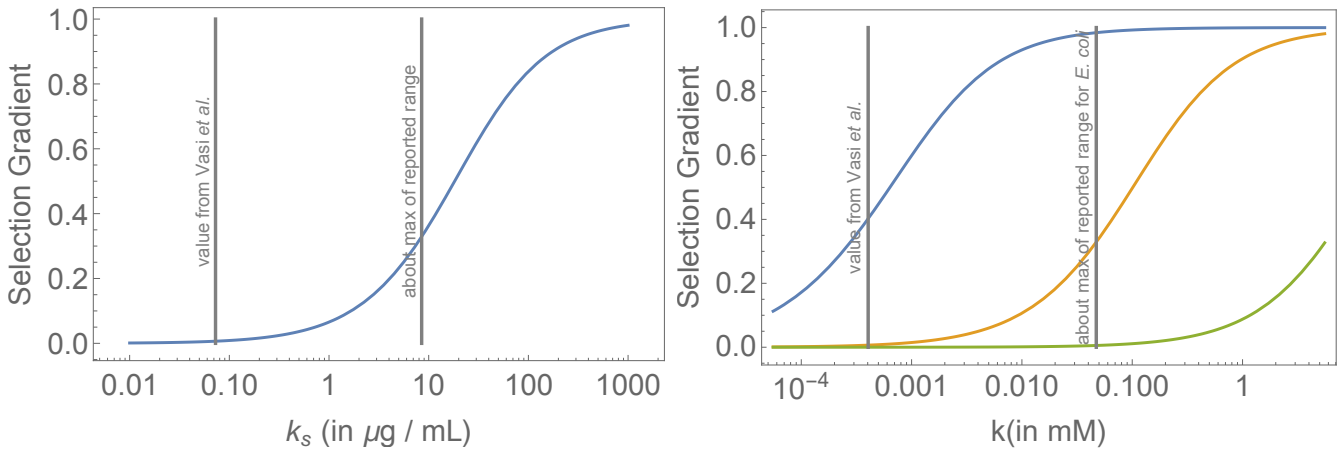

Figure A.2: Dependency of the selection gradient on the k_s in the LTEE set-up and different setups. We have taken the selection gradient for a decrease in k (minus the selection gradient) for ecstatical purposes. Range of k_S values taken from[22]. Orange is LTEE conditions, green 100x higher substrate, blue 100x lower substrate.

$$
\begin{aligned}
S_\mu &= \frac{\mu^*}{W^*}\frac{\partial W^*}{\partial \mu^*}(\mu^* = \mu) = 1 \\
S_y &= \frac{y^*}{W^*}\frac{\partial W^*}{\partial y^*}(y^* = y) = 0 \\
S_k &= \frac{k^*}{W^*}\frac{\partial W^*}{\partial k^*}(k^* = k) = \frac{-k\left(1 + \frac{\ln\left(\frac{k+s_0}{k}\right)}{\ln\left(\frac{x_0+ys_0}{x_0}\right)}\right)}{k + \frac{x_0}{y} + s_0}
\end{aligned}
\tag{26}
$$

Using this equation, we can calculate selection on the Monod constant in an experimental setting. For the Long Term Evolution Experiment (values from[9]) we find $S_k = -0.00657233$, which agrees with the -0.0066 mentioned in the paper, where they obtain this result with numerical calculations). As this selection gradient is very low (compared to $S_\mu = 1$)—and indeed they do not observe any increase in the affinity over the course of evolution —, we wondered if we expect to see selection on the Monod constant for different strains for *E. coli* or under different condition. Higher values for k lead to a higher selection gradient, and the k for *E. coli* strains a factor 100 higher than the value of 0.727 $\mu g/mL$ reported for REL606[9]. At those higher values we can see that the selection of the k_S does become important, as well as under different experimental conditions (see Figure A.2). Selection on the k_S might be more important for other substrates or other organisms, e.g. if uptake is not active but based on a diffusion gradient such as for the yeast *Saccharomyces cerevisiae* the k_S is usually (much) higher.

The landscape of invasion fitness and the gradient of this landscape (the selection gradient) can be visualized (Fig. A.3). S_k is always lower or equal to S_μ, which has implications for a k/μ trade-off, namely that the trade-off is only relevant if a 1% effect on the maximal growth rate has a bigger than 1% effect on the k_s.

When we plot the selection coefficient and the trade-off function for a resident in the Long Term Evolution experiment[9] we see that we still expect the selection to be almost completely on increasing the maximum growth rate (Figure A.3left top). We see similar results when we use a trade-off based on enzyme kinetics[16] (Figure A.3right top). However, when we would repeat the experiment with a 100 times lower starting glucose concentration, we would expect a much more pronounced selection on the affinity (Figure A.3bottom).

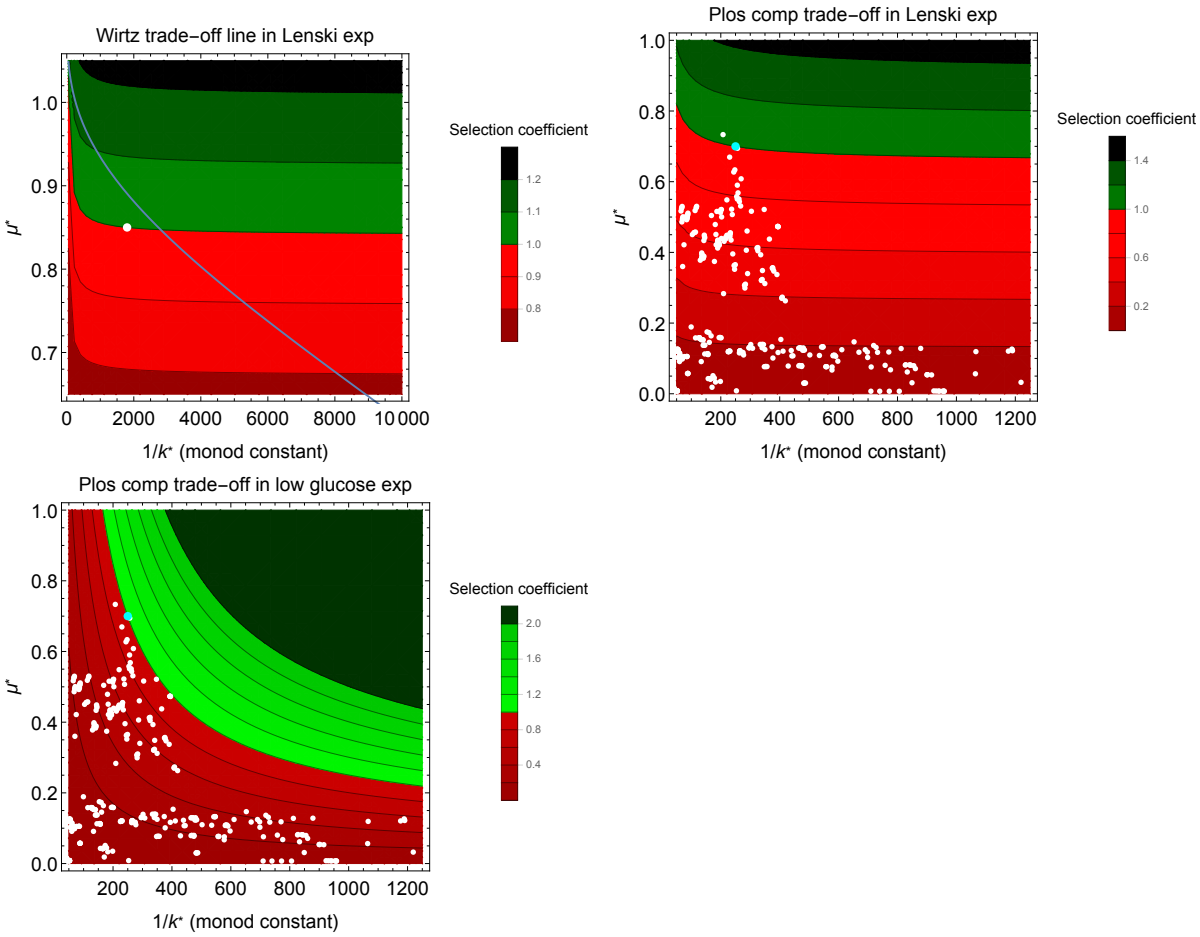

Figure A.3: **Landscapes of invasion fitness (selection coefficient) for different conditions.** The selection gradient is the slope in this landscape. **Left top** Tradeoff from[14] with conditions from the Long Term Evolution Experiment[9]. Selection mostly promotes maximum growth rate. **Right top** Tradeoff from[16] with the same conditions give similar results. **Bottom** When initial glucose is 100 times lower, the trade-off has a pronounced effect and selection acts both on the maximal growth rate and the affinity.

A.5 Invasive potential for different species, trade-offs and experimental conditions

See figures A.4 and A.5

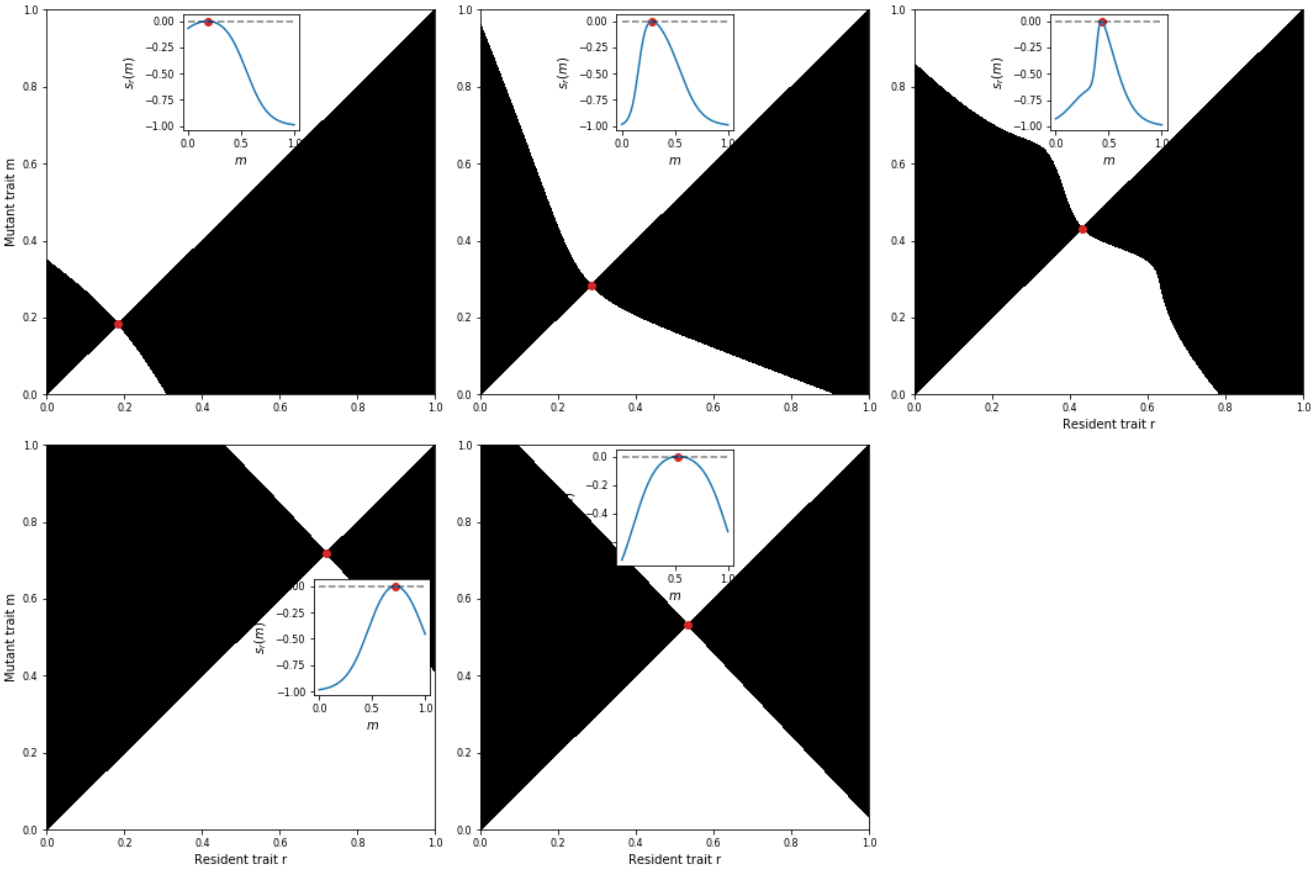

Figure A.4: **Pairwise invasibility plots for the different trade-offs** Top row: different trade-offs for *E. coli* (experimental fit, computational fit and computational fit anaerobic) with experimental conditions: initial glucose = 0.1375 mM and initial cells are $0.5{\cdot}10^6$ cells/ml. Bottom row: different trade-offs for *S. cerevisiae* (experimental fit and computational fit) with experimental conditions: initial glucose = 100 mM and initial cells are $0.1{\cdot}10^6$ cells/ml. For *S. cerevisiae* k_S runs from 0.1 to 100 for u from 0 to 1.

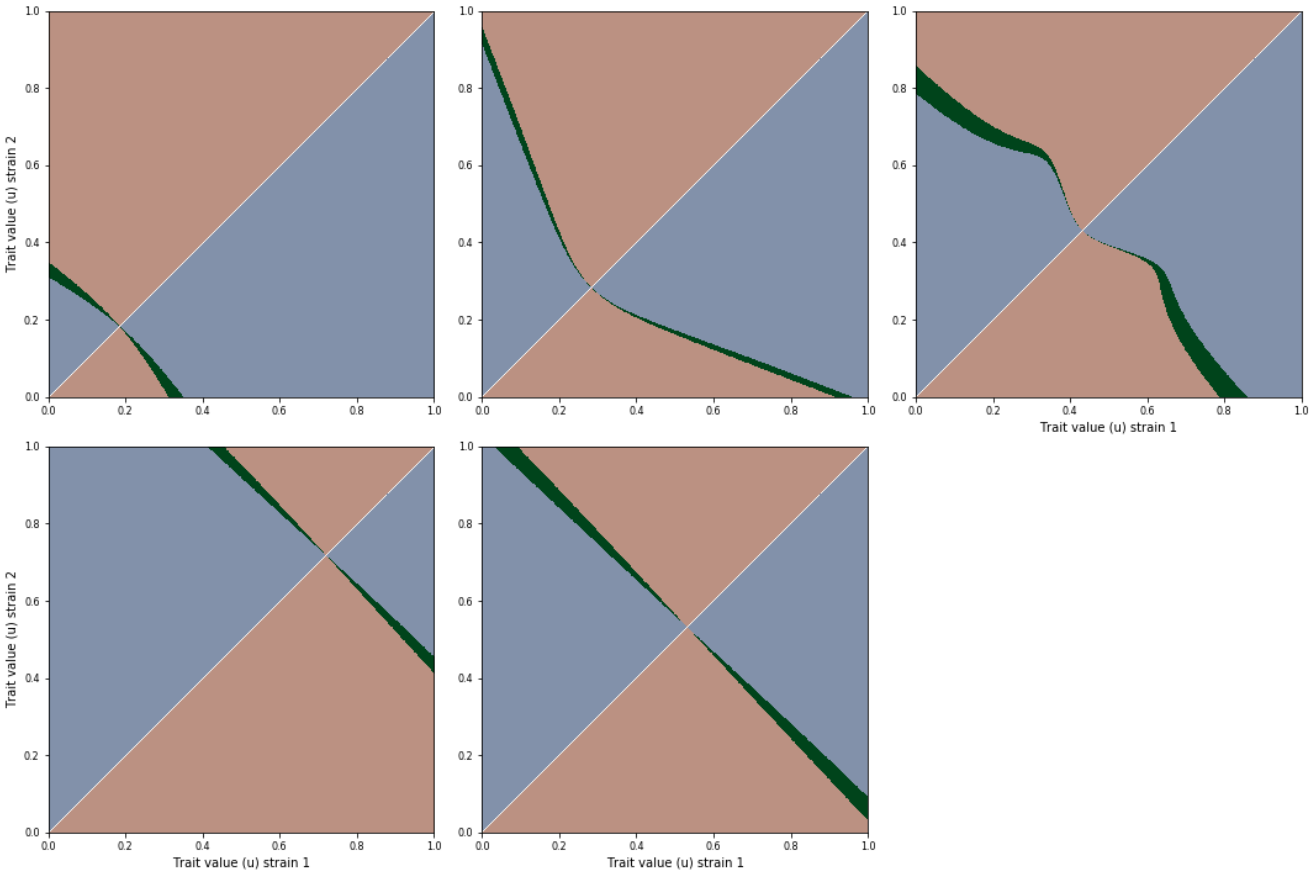

Figure A.5: **Areas of coexistence for the different trade-offs** Top row: different trade-offs for *E. coli* (experimental fit, computational fit and computational fit anaerobic) with experimental conditions: initial glucose = 0.1375 mM and initial cells are $0.5{\cdot}10^6$ cells/ml. Bottom row: different trade-offs for *S. cerevisiae* (experimental fit and computational fit) with experimental conditions: initial glucose = 100 mM and initial cells are $0.1{\cdot}10^6$ cells/ml. For *S. cerevisiae* k_S runs from 0.1 to 100 for u from 0 to 1.

A.6 Stochastic simulations

When integrating the trade-off in our models we have chosen a 'specialization parameter' u, that runs from 0 (specialization on low resource) to 1 (specialization on high resource). The general conversion is:

$$k = k_{min} 10^{u \log_{10}\left(\frac{k_{max}}{k_{min}}\right)} \tag{27}$$

We have used the trade-off described in the main text to determine μ_{max} and $Y_{X/S}$ from u. For the simulations, we allowed for 51 different phenotypes at one time, and tracked their fractions at the beginning and end of a fluctuation to determine the relative growth rate of a phenotype. All growing phenotypes could generate offspring with small but stochastic mutations, with a small chance, whenever free phenotypes were available. We simulated these systems until a stable phenotype distribution was reached (Figure A.6).

To plot the phenotype trajectories in Figure 4, we needed to convert the collection of phenotypes to one or two main trait values. We did this by taking only the phenotypes which had a density of more than 1/1000th of more abundant phenotype. Then we checked if all those phenotypes were close together or far apart, and created either one or two groups. For every group we took the weighted mean to determine the consensus phenotype. See Figure A.7 for two examples of the outcome of this algorithm.

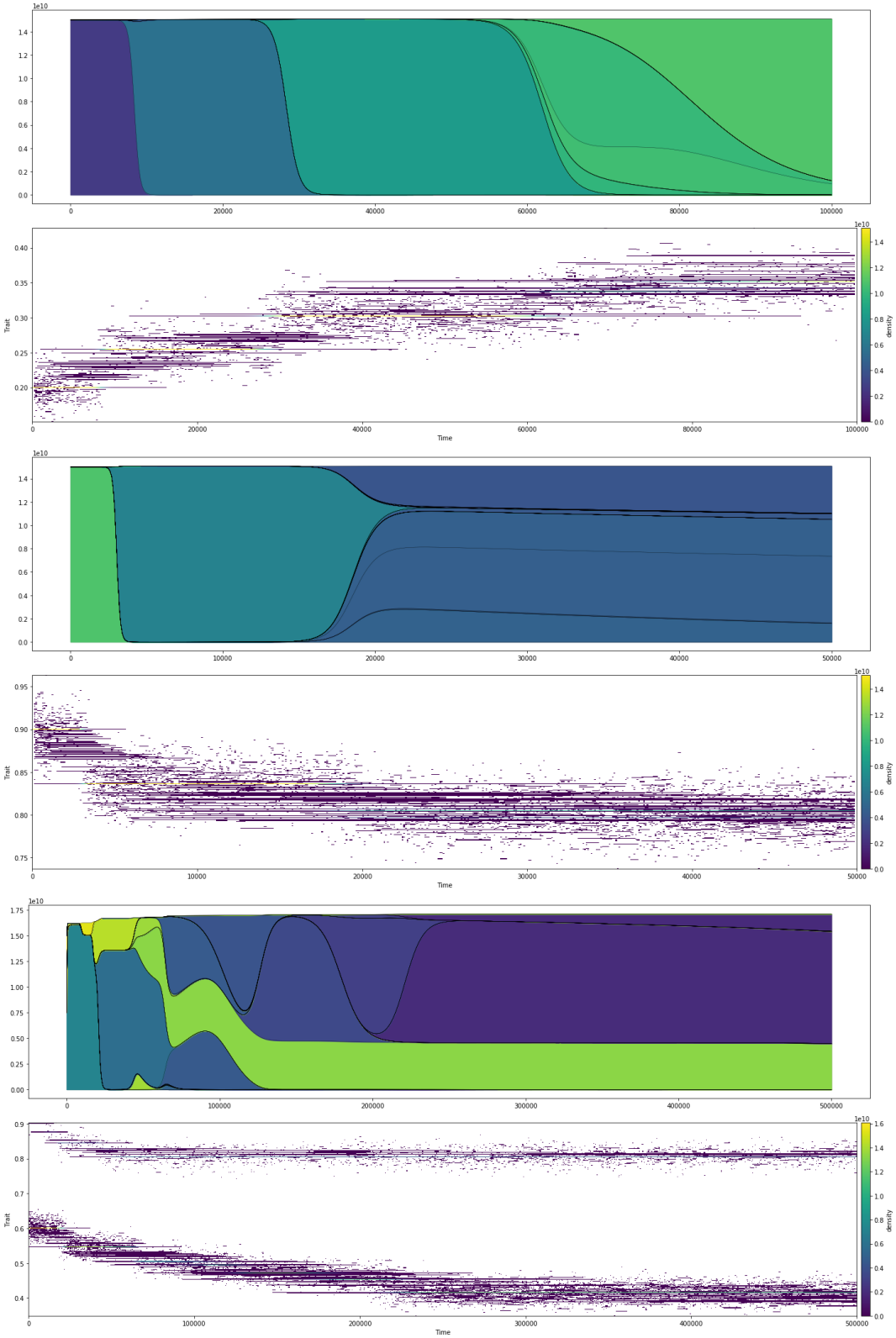

Figure A.6: Trajectories of stochastic simulations starting from different initial conditions

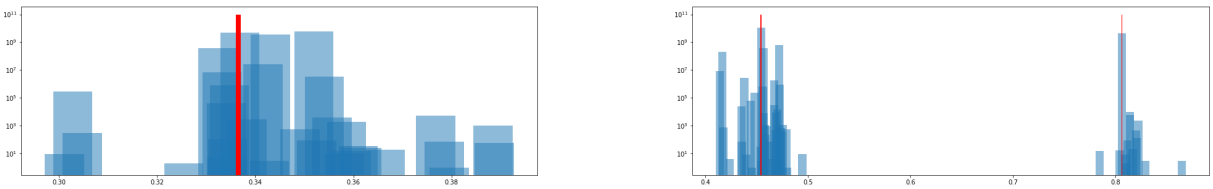

Figure A.7: The red line(s) show(s) the traits used for plotting the trajectories on the protected polymorphisms plot for two different examples (left: with 1 type. Right: with two types)